SANDIA REPORT

SAND2002-3614
Unlimited Release
Printed November 2002

Tangential Velocity Measurement using Interferometric MTI Radar

Armin W. Doerry, Brian P. Mileshosky, and Douglas L. Bickel

Prepared by
Sandia National Laboratories
Albuquerque, New Mexico 87185 and Livermore, California 94550

Sandia is a multiprogram laboratory operated by Sandia Corporation, a Lockheed Martin Company, for the United States Department of Energy under Contract DE-AC04-94AL85000.

Issued by Sandia National Laboratories, operated for the United States Department of Energy by Sandia Corporation.

Available to DOE and DOE contractors from
U.S. Department of Energy
Office of Scientific and Technical Information
P.O. Box 62
Oak Ridge, TN 37831

Telephone: (865)576-8401
Facsimile: (865)576-5728
E-Mail: reports@adonis.osti.gov
Online ordering: http://www.doe.gov/bridge

Available to the public from
U.S. Department of Commerce
National Technical Information Service
5285 Port Royal Rd
Springfield, VA 22161

Telephone: (800)553-6847
Facsimile: (703)605-6900
E-Mail: orders@ntis.fedworld.gov
Online order: http://www.ntis.gov/ordering.htm

SAND2001-3614
Unlimited Release
Printed November 2002

Tangential Velocity Measurement using Interferometric MTI Radar

Armin W. Doerry, Brian P. Mileshosky, and Douglas L. Bickel
Radar and Signals Analysis Department
Sandia National Laboratories
PO Box 5800
Albuquerque, NM 87185-0519

ABSTRACT

An Interferometric Moving Target Indicator radar can be used to measure the tangential velocity component of a moving target. Multiple baselines, along with the conventional radial velocity measurement, allow estimating the true 3-D velocity vector of a target.

ACKNOWLEDGEMENTS

This work was funded by the US DOE National Nuclear Security Administration, Office of Defense Nuclear Nonproliferation, Office of Nonproliferation Research and Engineering (NNSA/NA-22), under the Advanced Radar System (ARS) project. This effort is directed by Randy Bell.

CONTENTS

This page left intentionally blank.

1. Introduction & Background

Radar systems use time delay measurements between a transmitted signal and its echo to calculate range to a target. Ranges that change with time cause a Doppler offset in phase and frequency of the echo. Consequently, the closing velocity between target and radar can be measured by measuring the Doppler offset of the echo. The closing velocity is also known as radial velocity, or line-of-sight velocity. Doppler frequency is measured in a pulse-Doppler radar as a linear phase shift over a set of radar pulses during some Coherent Processing Interval (CPI).

Radars that detect and measure target velocity are known as Moving-Target-Indicator (MTI) radars. MTI radars that are operated from aircraft are often described as Airborne-MTI (AMTI) radars. When AMTI radars are used to detect and measure ground-based moving-target vehicles, they are often described as Ground-MTI (GMTI) radars. Good introductions to MTI radar operation are given in texts by Skolnik[1] and Nathanson.[2]

In MTI radars, the angular direction of a target is presumed to be in the direction to which the antenna is pointed. Consequently, a MTI radar generally offers fairly complete position information (angular direction and range) to some degree of precision, but incomplete velocity information since Doppler is proportional to the time-rate-of-change of range, i.e. radial velocity. Tangential velocities, that is, velocities normal to the range direction do not cause a Doppler shift, so are not measured directly. Tangential velocities can be measured indirectly by tracking the angular position change with time, but this requires a somewhat extended viewing time for any degree of accuracy and/or precision.

Of course, multiple MTI systems might be employed in concert, each measuring radial velocities in different spatial directions. In this manner, a two-dimensional (or even full three-dimensional) target velocity vector may be estimated. This is the basic concept behind DARPA's AMSTE program.[3] However, this technique requires that the radars be widely separated to facilitate the necessary triangulation (e.g. on different aircraft in the case of GMTI systems).

GMTI systems are often employed from moving radar platforms such as aircraft, that is, the radar itself is in motion with respect to the ground. Consequently, the stationary ground itself offers Doppler frequency shifts. In addition, since different areas of the ground are within view of different parts of the antenna beam, and have somewhat different radial velocities, the ground offers a spectrum of Doppler frequencies to the radar. This is often referred to as the clutter spectrum, and can mask the Doppler returns for slow-moving target vehicles of interest. Of course, if a target's Doppler is outside of the clutter spectrum, its detection and measurement are relatively easy. This is called "exoclutter" GMTI operation. Detecting and measuring echo responses from slow-moving target vehicles that are masked by the clutter is considerably more difficult, and is called "endoclutter" GMTI operation.

The ability to observe targets masked by clutter is often called “sub-clutter visibility”. Reducing the effects of clutter on detecting and measuring such targets’ motion is often termed “clutter suppression”. This is most often accomplished by employing multiple antennas on a single aircraft arrayed along the flight direction of the radar, and is often called a Displaced Phase Center Antenna (DPCA) technique, or Interferometric GMTI.[4,5,6,7,8] Interferometric techniques allow making independent angle measurements not affected by target motion, thereby facilitating discrimination of a moving vehicle in one part of the antenna beam from clutter in another part of the antenna beam that otherwise exhibits identical Doppler signatures. Interferometers might be constructed from separate distinct antennas, or from monopulse antennas that offer the equivalent of separate distinct antenna phase centers in a single structure. Good introductions to monopulse antenna operation and interferometers are presented in Skolnik[1] and Mahafza[9].

Nevertheless, tangential velocity measurements within a single CPI remain problematic, and in fact unaddressed in the literature. However, the need for a more complete target velocity vector of a time-critical moving vehicle, as measured from a single aircraft, remains.

2. Overview & Summary

A radar interferometer can measure angular position to a target with a great deal of precision, even with a single radar pulse. It does so by measuring the phase difference between echoes arriving at the two antennas. A target with tangential velocity will exhibit a pulse-to-pulse change in the angular position as measured by the phase difference between the antennas. This manifests itself as an interferometric phase that changes with time, i.e. a Doppler difference frequency. By measuring this difference frequency over some CPI, a tangential velocity can be calculated for the target. This tangential velocity will be in the direction of the interferometric baseline. Consequently, a multiple orthogonal baseline arrangement can measure tangential velocities in both the azimuth and elevation directions. These coupled with the radial velocity derived from traditional Doppler processing enables a full 3-dimensional velocity vector to be measured from a single CPI.

Subaperture techniques allow for filtering individual Doppler returns when multiple moving targets exist at the same range.

This technique is usable for a wide variety of radar systems applications, including air traffic control, ground vehicle target tracking, law-enforcement, and traffic monitoring and control. This technique also extends to other coherent remote sensing systems such as sonar, ultrasound, and laser systems.

3. Detailed Analysis

Consider a monostatic radar employing a Linear-FM chirp, stretch-processing, and quadrature demodulation. It is then well-known that the return echo exhibits a sampled video phase that may be adequately described by

$$\Phi_V(i,n) = \frac{2}{c}\left(w + gT_s i\right)\left(|\mathbf{r}_c| - |\mathbf{r}_s|\right) \tag{1}$$

where

c = velocity of propagation,
w = radar center frequency,
g = radar chirp rate,
T_s = Analog to Digital conversion period (sampling period),
i = intra-pulse sampling index with $-I/2 < i \le I/2$,
n = inter-pulse index with $-N/2 < n \le N/2$,
$\mathbf{r}_c$ = vector from target reference location to radar,
$\mathbf{r}_s = \mathbf{r}_c - \mathbf{s}$ = vector from target exhibiting radar echo to radar, and
$\mathbf{s}$ = vector from target reference location to target exhibiting radar echo.

One development of this expression is given by Doerry.[10] The geometry is illustrated in figure 1.

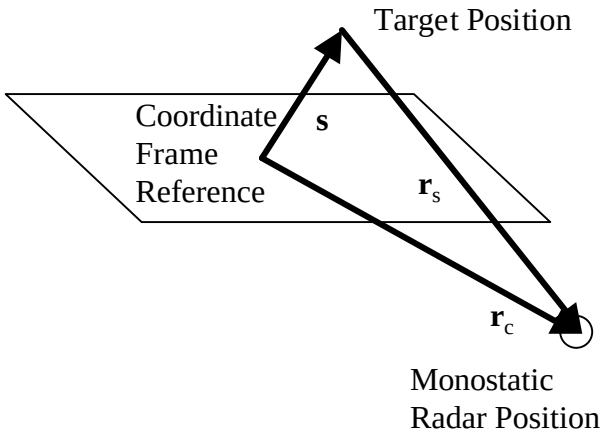

Figure 1. Monostatic Radar geometry.

Vectors $\mathbf{r}_c$ and $\mathbf{s}$ will be presumed to be able to change with index *n*. The signal itself will have some amplitude *A*, and with this phase can be described by

$$X_V(i,n) = Ae^{j\Phi_V(i,n)}. \tag{2}$$

The phase is adequately approximated by

$$\Phi_V(i,n) = \frac{2}{c}(w + gT_s i)\frac{\mathbf{r}_c \circ \mathbf{s}}{|\mathbf{r}_c|}. \tag{3}$$

If a second receive-only antenna is located with a baseline vector **b** with respect to the original transmit/receive antenna, with geometry illustrated in figure 2, then its bistatic return echo exhibits a video phase described by

$$\Phi_{V,\mathbf{b}}(i,n) = \frac{1}{c}(w + gT_s i)\left(|\mathbf{r}_c + (\mathbf{r}_c + \mathbf{b})| - |\mathbf{r}_s + (\mathbf{r}_s + \mathbf{b})|\right) \tag{4}$$

which for small baseline lengths is adequately approximated by

$$\Phi_{V,\mathbf{b}} = \frac{2}{c}(w + gT_s i)\left(\frac{\mathbf{r}_c \circ \mathbf{s}}{|\mathbf{r}_c|} + \frac{\mathbf{b} \circ \mathbf{s}}{2|\mathbf{r}_c|}\right). \tag{5}$$

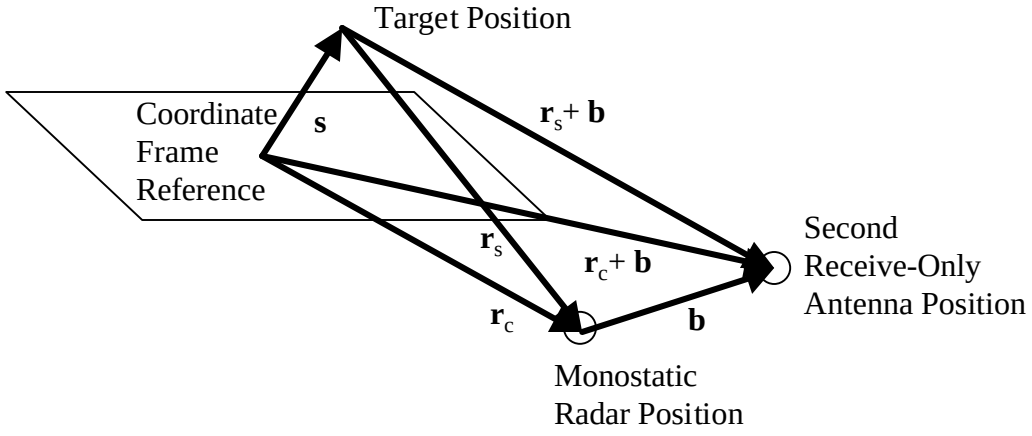

Figure 2. Dual antenna interferometer geometry.

The video signal that exhibits this phase can be described by

$$X_{V,\mathbf{b}}(i,n) = Ae^{j\Phi_{V,\mathbf{b}}(i,n)}. \tag{6}$$

We note that when $|\mathbf{b}| = 0$ this reduces to the monostatic case.

A moving target implies that target location vector **s** changes from radar pulse to pulse as

$$\mathbf{s} = \mathbf{s}_0 + \mathbf{v}_s T_p n \tag{7}$$

where

$\mathbf{s}_0$ = target reference position at $n = 0$,
$\mathbf{v}_s$ = target velocity vector, and
T_p = Pulse Repetition Interval (PRI).

In general the radar itself can be moving, i.e. changing position from pulse to pulse as

$$\mathbf{r}_c = \mathbf{r}_{c0} + \mathbf{v}_c T_p n \tag{8}$$

where

$\mathbf{r}_0$ = radar reference position at $n = 0$, and
$\mathbf{v}_c$ = radar velocity vector.

Assuming a constant baseline vector, this allows expansion to the approximation

$$\Phi_{V,\mathbf{b}}(i,n) = \frac{2}{c}(w + gT_s i)\left(\begin{array}{l}\left(\frac{\mathbf{r}_{c0}\circ\mathbf{s}_0}{|\mathbf{r}_{c0}|} + \frac{\mathbf{b}\circ\mathbf{s}_0}{2|\mathbf{r}_{c0}|}\right) + \left(\frac{\mathbf{r}_{c0}\circ\mathbf{v}_s}{|\mathbf{r}_{c0}|} + \frac{\mathbf{v}_c\circ\mathbf{s}_0}{|\mathbf{r}_{c0}|} + \frac{\mathbf{b}\circ\mathbf{v}_s}{2|\mathbf{r}_{c0}|}\right)T_p n \\ + \left(\frac{\mathbf{v}_c\circ\mathbf{v}_s}{|\mathbf{r}_{c0}|}\right){T_p}^2 n^2\end{array}\right). \tag{9}$$

Typical GMTI parameters are such that this can usually be further simplified to the approximation

$$\Phi_{V,\mathbf{b}}(i,n) = \left\{\begin{array}{l}\frac{2gT_s}{c}\left(\frac{\mathbf{r}_{c0}\circ\mathbf{s}_0}{|\mathbf{r}_{c0}|} + \frac{\mathbf{b}\circ\mathbf{s}_0}{2|\mathbf{r}_{c0}|}\right)i \quad + \quad \frac{2wT_p}{c}\left(\frac{\mathbf{r}_{c0}\circ\mathbf{v}_s}{|\mathbf{r}_{c0}|} + \frac{\mathbf{v}_c\circ\mathbf{s}_0}{|\mathbf{r}_{c0}|} + \frac{\mathbf{b}\circ\mathbf{v}_s}{2|\mathbf{r}_{c0}|}\right)n \\ \quad + \quad \frac{2w}{c}\left(\frac{\mathbf{b}\circ\mathbf{s}_0}{2|\mathbf{r}_{c0}|}\right)\end{array}\right\}. \tag{10}$$

Note that we are ignoring some constant phase terms that are inconsequential to target position and motion estimation.

This phase is of a form

$$\Phi_{V,\mathbf{b}}(i,n) = \quad w_i i \quad + \quad w_n n \quad + \quad j \tag{11}$$

where

$$w_i = \frac{2gT_s}{c}\left(\frac{\mathbf{r}_{c0}\circ\mathbf{s}_0}{|\mathbf{r}_{c0}|}+\frac{\mathbf{b}\circ\mathbf{s}_0}{2|\mathbf{r}_{c0}|}\right),$$

$$w_n = \frac{2wT_p}{c}\left(\frac{\mathbf{r}_{c0}\circ\mathbf{v}_s}{|\mathbf{r}_{c0}|}+\frac{\mathbf{v}_c\circ\mathbf{s}_0}{|\mathbf{r}_{c0}|}+\frac{\mathbf{b}\circ\mathbf{v}_s}{2|\mathbf{r}_{c0}|}\right), \text{ and}$$

$$j = \frac{2w}{c}\left(\frac{\mathbf{b}\circ\mathbf{s}_0}{2|\mathbf{r}_{c0}|}\right).$$

Note also that we have three principal terms. The first is a coefficient of index *i*, and represents a frequency with respect to index *i*. The second is a coefficient of index *n*, and represents a frequency with respect to index *n*. The third is a constant phase term with respect to indices *i* and *n*. A complete MTI data set corresponds to a data array of size *N* x *I*, with elemental positions denoted by indices *n* and *i*.

The coefficient of index *i* can be identified via a Fourier Transform of the video signal data over index *i*. The coefficient of index *n* can be identified via a Fourier Transform of the video signal data over index *n*. Performing Fourier Transforms across both indices *i* and *n* yields a range-Doppler map, where peak responses in the map indicate targets at a specific range and velocity. That is, the range-Doppler map is described by

$$Z_{\mathbf{b}}(v,u) = \Im_n\left(\Im_i\left(X_V(i,n)\right)\right) = \sum_n\sum_i X_V(i,n)e^{-jw_v i}e^{-jw_u n} = A\,W_v(w_v - w_i)W_u(w_u - w_n)e^{jj} \tag{12}$$

where

v = the range index of the range-Doppler map with $-V/2 < v \le V/2$,
u = the Doppler index of the range-Doppler map with $-U/2 < v \le U/2$,
w_v = the map's range scale value corresponding to index v,
w_u = the map's Doppler scale value corresponding to index u,
$W_v(\ )$ = the map's range impulse response function, with peak at $W_v(0)$, and
$W_u(\ )$ = the map's Doppler impulse response function, with peak at $W_u(0)$.

We define the range-Doppler map for the monostatic case as

$$Z_0(v,u) = Z_{\mathbf{b}}(v,u)\big|_{\mathbf{b}=0}. \tag{13}$$

We now define a coordinate frame with unit vectors

$\hat{\mathbf{r}} = -\mathbf{r}_{c0}/|\mathbf{r}_{c0}|$ = range direction, such that $\mathbf{r}_{c0} = -|\mathbf{r}_{c0}|\hat{\mathbf{r}}$,
$\hat{\mathbf{a}}$ = azimuth direction vector, horizontal, to the right, and orthogonal to $\hat{\mathbf{r}}$, and
$\hat{\mathbf{e}} = \hat{\mathbf{a}}\times\hat{\mathbf{r}}$ = elevation direction vector.

Tangential velocities are in the azimuth and/or elevation directions and are embodied in the $\mathbf{b} \circ \mathbf{v}_s$ term.

We also define the vector quantities in this frame as

$$\begin{aligned}
\mathbf{r}_{c0} &= -|\mathbf{r}_{c0}|\hat{\mathbf{r}} \\
\mathbf{v}_c &= v_{cr}\hat{\mathbf{r}} + v_{ca}\hat{\mathbf{a}} + v_{ce}\hat{\mathbf{e}} \\
\mathbf{s}_0 &= s_r\hat{\mathbf{r}} + s_a\hat{\mathbf{a}} + s_e\hat{\mathbf{e}} \\
\mathbf{v}_s &= v_{sr}\hat{\mathbf{r}} + v_{sa}\hat{\mathbf{a}} + v_{se}\hat{\mathbf{e}} \\
\mathbf{b} &= b_r\hat{\mathbf{r}} + b_a\hat{\mathbf{a}} + b_e\hat{\mathbf{e}}
\end{aligned} \tag{14}$$

We can then write a somewhat simplified

$$\Phi_{V,\mathbf{b}}(i,n) = \left\{ \begin{array}{l} \dfrac{2gT_s}{c}\left(-s_r + \dfrac{\mathbf{b}\circ\mathbf{s}_0}{2|\mathbf{r}_{c0}|}\right)i \quad + \quad \dfrac{2wT_p}{c}\left(-v_{sr} + \dfrac{\mathbf{v}_c\circ\mathbf{s}_0}{|\mathbf{r}_{c0}|} + \dfrac{\mathbf{b}\circ\mathbf{v}_s}{2|\mathbf{r}_{c0}|}\right)n \\ \quad + \quad \dfrac{2w}{c}\left(\dfrac{\mathbf{b}\circ\mathbf{s}_0}{2|\mathbf{r}_{c0}|}\right) \end{array} \right\}. \tag{15}$$

Exoclutter GMTI

Exoclutter GMTI generally is monostatic (no baseline is relevant). Furthermore, it assumes that (or resigns itself to the case where) target radial velocity offers Doppler shifts much greater than the clutter spectrum width, namely $|v_{sr}| >> |\mathbf{v}_c \circ \mathbf{s}_0|/|\mathbf{r}_{c0}|$. Consequently the model for target phase becomes

$$\Phi_{V,\mathbf{b}}(i,n) = \frac{2gT_s}{c}(-s_r)i \quad + \quad \frac{2wT_p}{c}(-v_{sr})n\,. \tag{16}$$

The processing of this signal is outlined in figure 3.

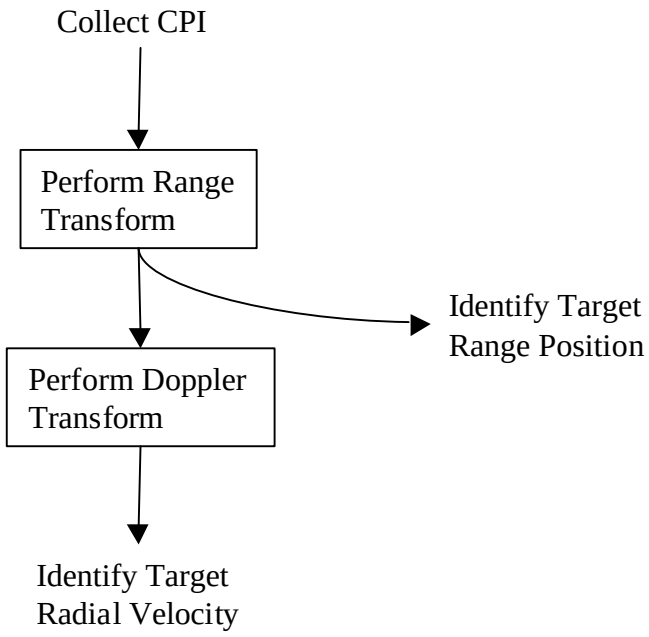

Figure 3. Processing steps for Exoclutter GMTI.

Target radial position is measured by a range transform across index *i*, and target radial velocity is measured with a Doppler transform across index *n*. That is, the range-Doppler map is approximately

$$Z_0(v,u) = A\,W_v\left(w_v - \frac{2gT_s}{c}(-s_r)\right)W_u\left(w_u - \frac{2wT_p}{c}(-v_{sr})\right). \qquad (17)$$

Endoclutter GMTI

Endoclutter GMTI uses interferometry with a baseline, and allows for measuring target radial velocities with Doppler shifts less than the clutter spectrum width, namely $|v_{sr}| < |\mathbf{v}_c \circ \mathbf{s}_0| / |\mathbf{r}_{c0}|$. The baseline is assumed to be small enough that it doesn't influence significantly the result of the Doppler transform across index *n*. Furthermore, the baseline is generally aligned in the azimuth direction, and horizontal radar flight path is presumed. Consequently, the model for target phase is presumed to be

$$\Phi_{V,\mathbf{b}}(i,n) = \frac{2gT_s}{c}(-s_r)i \quad + \quad \frac{2wT_p}{c}\left(-v_{sr} + \frac{v_{cr}s_r}{|\mathbf{r}_{c0}|} + \frac{v_{ca}s_a}{|\mathbf{r}_{c0}|}\right)n \quad + \quad \frac{2w}{c}\left(\frac{b_a s_a}{2|\mathbf{r}_{c0}|}\right) \qquad (18)$$

which is still in a form of equation (11), namely $\Phi_{V,\mathbf{b}}(i,n) = w_i i + w_n n + j$.

Processing steps for this model are outlined in figure 4.

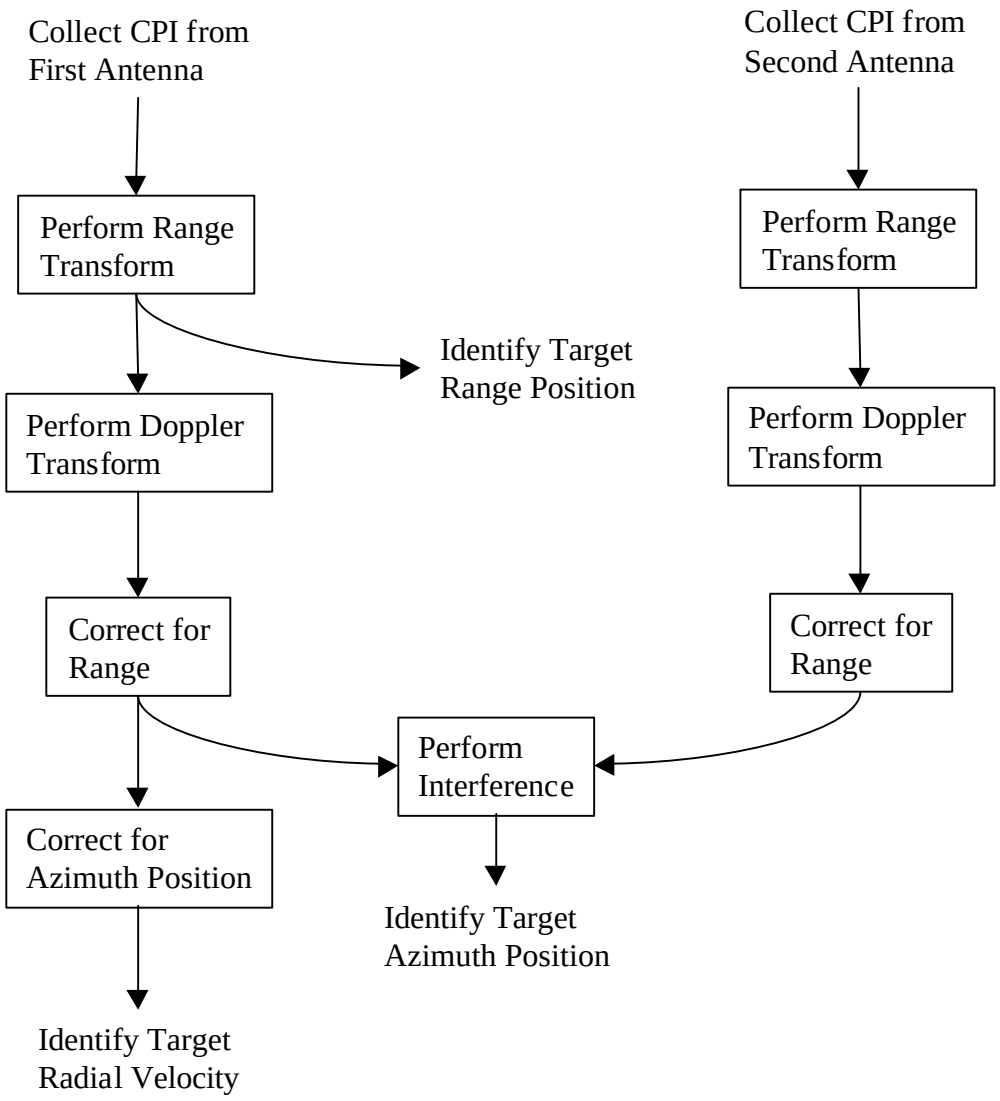

Figure 4. Processing steps for Endoclutter GMTI.

A range transform across index *i* allows identifying target radial position s_r. That is,

$$X_{R,\mathbf{b}}(v,n) = \Im_i\left(X_V(i,n)\right) = A\,W(w_v - w_i)e^{j\Phi_{R,\mathbf{b}}(v,n)} \tag{19}$$

where the remaining phase is

$$\Phi_{R,\mathbf{b}}(v,n) = \quad w_n n \quad + \quad j \ . \tag{20}$$

A Doppler transform across index *n* identifies w_n, which in turn identifies the quantity $\left(v_{sr} - v_{cr}s_r/|\mathbf{r}_{c0}| - v_{ca}s_a/|\mathbf{r}_{c0}|\right)$. That is, the range-Doppler map is described by

$$Z_{\mathbf{b}}(v,u) = \Im_n\left(X_{R,\mathbf{b}}(v,n)\right) = A\, W_v(w_v - w_i) W_u(w_u - w_n) e^{jj} \ . \tag{21}$$

Since s_r is known, its effects can be compensated to identify more specifically $\left(v_{sr} - v_{ca} s_a / |\mathbf{r}_{c0}|\right)$, but still leaves some ambiguity in resolving energy to some combination of the unknown quantities radial target velocity v_{sr} and target azimuth position s_a.

At this point we compare the range-Doppler maps made from both ends of the baseline. The monostatic antenna does not contain the baseline term in the above model, but the bistatic second antenna does contain this term. We compare the two results by interfering them to yield

$$IF(v,i) = Z_{\mathbf{b}}(v,u) Z_0{}^*(v,u) = \left|A\, W_v(w_v - w_i) W_u(w_u - w_n)\right|^2 e^{j\Delta f(v,u)} \tag{22}$$

where * denotes complex conjugate, and at each pixel

$$\Delta f(v,u) = \frac{2w}{c}\left(\frac{b_a s_a}{2|\mathbf{r}_{c0}|}\right). \tag{23}$$

Identifying this phase allows an independent estimate of target azimuth position s_a, which can then be used to correct the result of the earlier Doppler transform result to uniquely identify target radial velocity v_{sr}. These quantities have thereby been separated, or discriminated.

A key point here is that the baseline's influence is analyzed only after the complete range-Doppler maps are formed for both receiving antennas.

Simple Stationary MTI for Estimating Tangential Velocity

We now investigate a simple example to illustrate the concept of extracting tangential velocity information. Consider a stationary interferometric radar ($\mathbf{v}_c = 0$) with baseline oriented in the azimuth direction. The model for target phase becomes

$$\Phi_{V,\mathbf{b}}(i,n) = \frac{2gT_s}{c}\left(-s_r + \frac{b_a s_a}{2|\mathbf{r}_{c0}|}\right)i \ + \ \frac{2wT_p}{c}\left(-v_{sr} + \frac{b_a v_{sa}}{2|\mathbf{r}_{c0}|}\right)n \ + \ \frac{2w}{c}\left(\frac{b_a s_a}{2|\mathbf{r}_{c0}|}\right). \tag{24}$$

The processing steps for this model are outlined in figure 5.

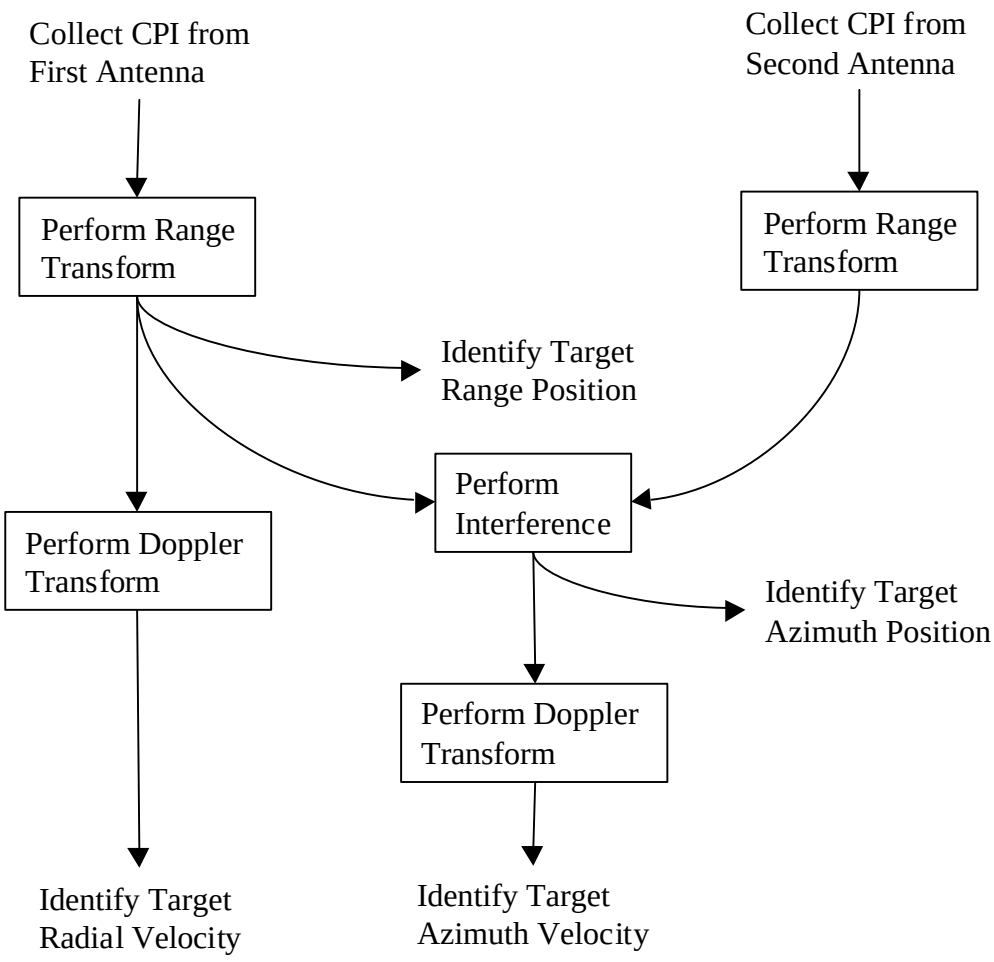

Figure 5. Processing steps for simple estimation of tangential velocity.

A range transform across index *i* allows identifying target radial position s_r, and leaves the data with a residual phase

$$\Phi_{R,\mathbf{b}} = \frac{2wT_p}{c}\left(-v_{sr} + \frac{b_a v_{sa}}{2|\mathbf{r}_{c0}|}\right)n \quad + \quad \frac{2w}{c}\left(\frac{b_a s_a}{2|\mathbf{r}_{c0}|}\right). \tag{25}$$

Target radial velocity can be estimated from the monostatic antenna data in the usual manner. If, however, this range-compressed data from each of the two antennas is interfered with each other, that is, a phase comparison is made before any Doppler transform, then resultant data is expressed as

$$IF_R(v,n) = \left|AW(w_v - w_n)\right|^2 e^{j\Delta f(v,n)} \tag{26}$$

where

$$\Delta f(v,n) = \frac{2wT_p}{c}\left(\frac{b_a v_{sa}}{2|\mathbf{r}_{c0}|}\right)n \quad + \quad \frac{2w}{c}\left(\frac{b_a s_a}{2|\mathbf{r}_{c0}|}\right). \tag{27}$$

Note that this interference signal with this phase characteristic is generated by point-by-point multiplication of the data from one range-compressed data set with the complex conjugate of the data from the other range-compressed data set.

The coefficient of index *n* in the phase is now a Doppler difference frequency that depends on target azimuth velocity v_{sa}. That is, for the interference signal now

$$w_n = \frac{2wT_p}{c}\left(\frac{b_a v_{sa}}{2|\mathbf{r}_{c0}|}\right). \tag{28}$$

A Doppler transform of this interference signal over index *n* now allows for identification of target azimuth velocity v_{sa} corresponding to the frequency content of the interference signal. That is, the range-Doppler map for this interference signal is now described by

$$Z_{IF}(v,u) = \Im_n(IF_R(v,n)) = |A\ W_v(w_v - w_i)|^2 W_u(w_u - w_n)e^{j\Delta f(v,0)} \tag{29}$$

where the 2-dimensional peak now describes target range and target tangential velocity. The average phase of the interference signal remains dependent on target azimuth position s_a, that is now

$$\Delta f(v,0) = \frac{2w}{c}\left(\frac{b_a s_a}{2|\mathbf{r}_{c0}|}\right). \tag{30}$$

In any case, the target tangential velocity in the azimuth direction v_{sa} can now also be identified.

The shortfall of this simplified technique is that it is very sensitive to noise, since the data that is interfered is only range compressed at that point, and doesn't benefit from the noise reduction offered by Doppler processing. Furthermore, multiple targets at the same range but at different radial velocities are indistinguishable from each other, and may in fact severely diminish the ability to find the correct tangential velocity for any one. Nevertheless, the concept of tangential velocity derived from interferometric MTI is herewith established.

More Robust Airborne GMTI Radar for Estimating Tangential Velocity

We now investigate a more complex scenario involving a moving radar. To not overly complicate the example, we limit elevation velocities to zero, and baseline orientation to the range-azimuth plane. Furthermore we will assume targets of interest exist in the exoclutter region. The complete phase model for the data is given by

$$\Phi_{V,\mathbf{b}}(i,n) = \left\{ \begin{array}{l} \dfrac{2gT_s}{c}\left(-s_r + \dfrac{\mathbf{b}\circ\mathbf{s}_0}{2|\mathbf{r}_{c0}|} \right) i \quad + \quad \dfrac{2wT_p}{c}\left(-v_{sr} + \dfrac{\mathbf{v}_c\circ\mathbf{s}_0}{|\mathbf{r}_{c0}|} + \dfrac{\mathbf{b}\circ\mathbf{v}_s}{2|\mathbf{r}_{c0}|} \right) n \\ \quad + \quad \dfrac{2w}{c}\left(\dfrac{\mathbf{b}\circ\mathbf{s}_0}{2|\mathbf{r}_{c0}|} \right) \end{array} \right\}. \tag{31}$$

The processing steps for this model are outlined in figure 6.

A range transform of the data across index *i* allows identifying target radial position s_r, and leaves the data with a residual phase

$$\Phi_{R,\mathbf{b}}(v,n) = \frac{2wT_p}{c}\left(-v_{sr} + \frac{v_{cr}s_r + v_{ca}s_a}{|\mathbf{r}_{c0}|} + \frac{b_r v_{sr} + b_a v_{sa}}{2|\mathbf{r}_{c0}|} \right) n + \frac{2w}{c}\left(\frac{b_r s_r + b_a s_a}{2|\mathbf{r}_{c0}|} \right). \tag{32}$$

We note that a function exhibiting some phase Θ perturbed by an undesired but known phase ε can be corrected by multiplying with a phase correction signal of unit amplitude and the negative of the phase perturbation. That is

$$\left(Ae^{j(\Theta+e)}\right)e^{-je} = Ae^{j(\Theta+e)-je} = Ae^{j\Theta}. \tag{33}$$

In this manner, since target radial position s_r is now known, the data can be corrected for its influence by applying a phase correction to yield

$$\Phi'_{R,\mathbf{b}}(v,n) = \Phi_{R,\mathbf{b}}(v,n) - \frac{2w}{c}\left(\frac{b_r s_r}{2|\mathbf{r}_{c0}|} \right) \tag{34}$$

or more explicitly

$$\Phi'_{R,\mathbf{b}}(v,n) = \frac{2wT_p}{c}\left(-v_{sr} + \frac{v_{ca}s_a}{|\mathbf{r}_{c0}|} + \frac{b_r v_{sr} + b_a v_{sa}}{2|\mathbf{r}_{c0}|} \right) n + \frac{2w}{c}\left(\frac{b_a s_a}{2|\mathbf{r}_{c0}|} \right). \tag{35}$$

At this point we split the CPI into two subapertures by dividing along index *n* to yield two new indices *m* and *k* such that

$$n = m + \left(k - \frac{1}{2} \right)\frac{N}{2} \tag{36}$$

where within a subaperture $-N/4 < m \le N/4$, and subaperture index *k* takes on values 0 or 1.

The range compressed data is now modeled with exhibiting phase

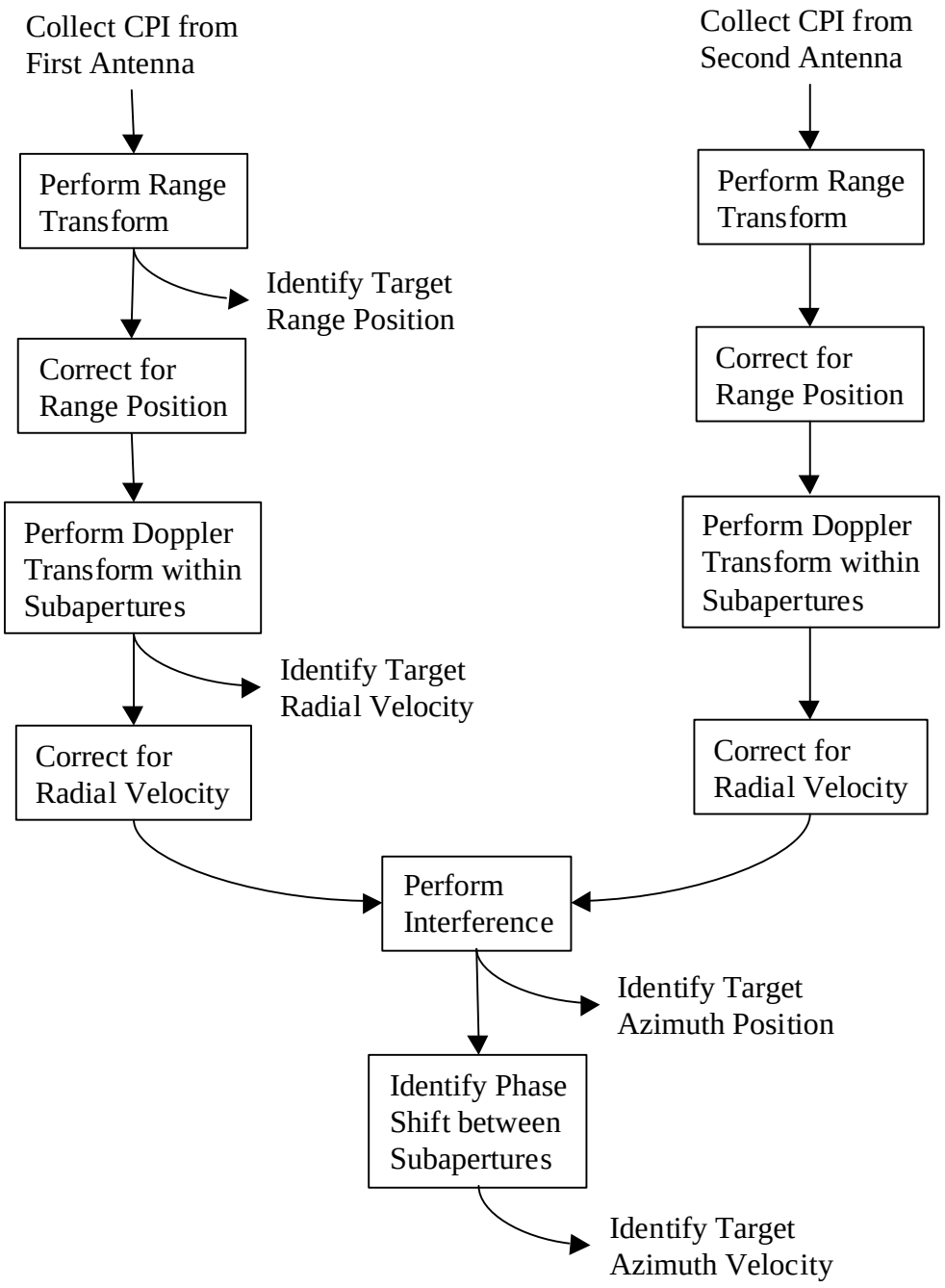

Figure 6. Processing steps for more robust airborne GMTI with tangential velocity estimation.

$$\Phi'_{R,\mathbf{b}}(v,m,k)= \left\{ \begin{array}{c} \frac{2wT_p}{c}\left(-v_{sr}+\frac{v_{ca}s_a}{|\mathbf{r}_{c0}|}+\frac{b_r v_{sr}+b_a v_{sa}}{2|\mathbf{r}_{c0}|}\right)m \\ +\frac{wT_pN}{c}\left(-v_{sr}+\frac{v_{ca}s_a}{|\mathbf{r}_{c0}|}+\frac{b_r v_{sr}+b_a v_{sa}}{2|\mathbf{r}_{c0}|}\right)k \\ +\frac{2w}{c}\left(\frac{b_a s_a}{2|\mathbf{r}_{c0}|}\right)-\frac{wT_pN}{2c}\left(-v_{sr}+\frac{v_{ca}s_a}{|\mathbf{r}_{c0}|}+\frac{b_r v_{sr}+b_a v_{sa}}{2|\mathbf{r}_{c0}|}\right) \end{array} \right\}. \quad (37)$$

Since we are dealing with exoclutter targets, a Doppler transform across index *m* yields an estimate of target radial velocity v_{sr} and a residual phase term

$$\Phi_{D,\mathbf{b}}(v,u,k)= \left\{ \begin{array}{c} \frac{wT_pN}{c}\left(-v_{sr}+\frac{v_{ca}s_a}{|\mathbf{r}_{c0}|}+\frac{b_r v_{sr}+b_a v_{sa}}{2|\mathbf{r}_{c0}|}\right)k \\ +\frac{2w}{c}\left(\frac{b_a s_a}{2|\mathbf{r}_{c0}|}\right)-\frac{wT_pN}{2c}\left(-v_{sr}+\frac{v_{ca}s_a}{|\mathbf{r}_{c0}|}+\frac{b_r v_{sr}+b_a v_{sa}}{2|\mathbf{r}_{c0}|}\right) \end{array} \right\}. \quad (38)$$

Since target radial velocity v_{sr} is now known, the data can be corrected for its influence by applying a phase correction to yield

$$\Phi'_{D,\mathbf{b}}(v,u,k)= \left\{ \begin{array}{c} \frac{wT_pN}{c}\left(\frac{v_{ca}s_a}{|\mathbf{r}_{c0}|}+\frac{b_a v_{sa}}{2|\mathbf{r}_{c0}|}\right)k \\ +\frac{2w}{c}\left(\frac{b_a s_a}{2|\mathbf{r}_{c0}|}\right)-\frac{wT_pN}{2c}\left(\frac{v_{ca}s_a}{|\mathbf{r}_{c0}|}+\frac{b_a v_{sa}}{2|\mathbf{r}_{c0}|}\right) \end{array} \right\}. \quad (39)$$

At this point we interfere the partially processed data from the two antennas on a point-by-point basis. This yields an interference signal result with phase given by

$$\Delta f(v,u,k)= \left\{ \frac{wT_pN}{c}\left(\frac{b_a v_{sa}}{2|\mathbf{r}_{c0}|}\right)k+\frac{2w}{c}\left(\frac{b_a s_a}{2|\mathbf{r}_{c0}|}\right)-\frac{wT_pN}{2c}\left(\frac{b_a v_{sa}}{2|\mathbf{r}_{c0}|}\right) \right\}. \quad (40)$$

This interference result still has two subapertures. The average phase allows estimation of target azimuth position s_a. If we now compare the phase of corresponding interference data across the two subapertures, that is across index *k*, we arrive at a phase difference measure of

$$\Delta(\Delta f(v,u,k))=\Delta f(v,u,1)-\Delta f(v,u,0)= \frac{wT_pN}{c}\left(\frac{b_a v_{sa}}{2|\mathbf{r}_{c0}|}\right) \quad (41)$$

which allows unique identification of target azimuth velocity v_{sa}. That is, the phase difference at each pixel of the corresponding subaperture interferograms is proportional to tangential velocity v_{sa}.

We note that in principle, splitting the CPIs into more than two subapertures prior to interfering them also allows extraction of tangential velocities.

Furthermore, a third receive-only antenna located with a second baseline vector oriented in the elevation direction would allow the additional discerning of the elevation-direction tangential velocity in a similar manner.

Accuracy and Precision of a Measurement

Interferometric measurements tend to be very sensitive to noise, and work best for targets with relatively high Signal-to-Noise Ratio (SNR). McDonough and Whalen[11] show that in this case, a phase difference can be measured to within an RMS error given by

$$s_{\Delta q} = \frac{1}{\sqrt{SNR}} \tag{42}$$

and a radian frequency can be measured to within an RMS error given by

$$s_{w} = \frac{1}{T\sqrt{SNR}} \tag{43}$$

where T is the RMS observation interval.

Consequently, for the more robust airborne GMTI described above, with two subapertures per antenna, the precision of the tangential velocity measurement can be calculated to be

$$s_{v_{sa}} = \left(\frac{c}{w}\right)\left(\frac{|\mathbf{r}_{c0}|}{b_a}\right)\frac{2}{T_p N\sqrt{SNR}} \tag{44}$$

where *SNR* refers to the results of the interference operation.

Example

As an example, consider an interferometric GMTI that has an antenna baseline spacing b_a = 3 m, and an operating frequency of 16.7 GHz. Furthermore, consider a target with an actual tangential velocity of 90 m/s at a range $|\mathbf{r}_{c0}|$ = 5 km, and SNR after interference is 100 (20 dB). With a CPI of T_pN = 0.25 s, we can calculate an expected precision of $s_{v_{sa}}$ = 3.8 m/s.

This result is from a single CPI. Of course tracking over multiple CPIs in the conventional manner will allow refinement.

4. Conclusions

The preceding development clearly shows the following points.

- Tangential velocities can be measured by an MTI radar by identifying the time dependence of the interferometric phase (phase difference) of an interferometric antenna pair, separated by a known baseline.

- Tangential velocity measurement requires interfering signals from at least two or more antennas prior to complete Doppler processing of the entire set of pulses from either antenna.

- Processing the CPIs from the respective antennas in two or more subapertures allows partial Doppler processing of each antenna's signals, but still allows interfering the result prior to completion of the Doppler processing.

- A three-dimensional velocity vector can be estimated by using 3 or more antennas that form at least two non-parallel baselines, with orthogonal components as viewed from the target location.

- This technique is applicable to ground-based MTI systems as well as airborne GMTI systems.

- This technique is applicable to any coherent imaging system.

References

[1] M. I. Skolnik, *Introduction to Radar Systems*, second edition, ISBN 0-07-057909-1, McGraw-Hill, Inc., 1980.

[2] F. E. Nathanson, *Radar Design Principles*, second edition, ISBN 0-07-046052-3, McGraw-Hill, Inc., 1990.

[3] D. R. Kirk, T. Grayson, D. Garren, C. Chong, "AMSTE precision fire control tracking overview", 2000 IEEE Aerospace Conference Proceedings, Big Sky, MT, USA, p.465-72 vol.3, 18-25 March 2000.

[4] M. A. Hasan, "Blind speed elimination for dual displaced phase center antenna radar processor mounted on a moving platform", US Patent 4,885,590, December 5, 1989.

[5] W. B. Goggins, "Method and apparatus for improving the slowly moving target detection capability of an AMTI synthetic aperture radar", US Patent 4,086,590, April 25, 1978.

[6] J. A. Didomizio, R, A. Guarino, "Dual cancellation interferometric AMTI radar", US Patent 5,559,516, September 24, 1996.

[7] J. A. DiDomizio, "Low target velocity interferometric AMTI radar", US Patent 5,559,518, September 24, 1996.

[8] E. F. Stockburger, H. D. Holt Jr., D. N. Held, R. A. Guarino, "Interferometric moving vehicle imaging apparatus and method", US Patent 5,818,383, October 6, 1998.

[9] B. R. Mahafza, *Introduction to Radar Systems*, ISBN 0-8493-1879-3, CRC Press, 1998.

[10] A. W. Doerry, "Patch Diameter Limitation due to High Chirp Rates in Focused SAR Images", IEEE Transactions on Aerospace and Electronic Systems, Vol. 30, No. 4, October 1994.

[11] R. N. McDonough, A. D. Whalen, *Detection of Signals in Noise*, second edition, ISBN 0-12-744852-7, Academic Press, 1995.

DISTRIBUTION

Unlimited Release

1	MS 0509	M. W. Callahan	2300
1	MS 0519	L. M. Wells	2344
1	MS 0519	D. L. Bickel	2344
1	MS 0519	J. T. Cordaro	2344
1	MS 0519	A. W. Doerry	2344
1	MS 0519	B. P. Mileshosky	2344
1	MS 0519	M. S. Murray	2344
1	MS 0519	S. D. Bensonhaver	2348
1	MS 0519	T. P. Bielek	2348
1	MS 0519	S. M. Devonshire	2348
1	MS 0519	W. H. Hensley	2348
1	MS 0519	J. A. Hollowell	2348
1	MS 0519	B. E. Mills	2348
1	MS 0519	A. L. Navarro	2348
1	MS 0519	J. W. Redel	2348
1	MS 0519	B. G. Rush	2348
1	MS 0519	G. J. Sander	2348
1	MS 0519	D. G. Thompson	2348
1	MS 0519	M. Thompson	2348
1	MS 0529	B. L. Remund	2340
1	MS 0529	B. L. Burns	2340
1	MS 0529	K. W. Sorensen	2345
1	MS 0529	B. C. Brock	2345
1	MS 0529	D. F. Dubbert	2345
1	MS 0529	S. S. Kawka	2345
1	MS 0529	G. R. Sloan	2345
1	MS 1207	C. V. Jakowatz, Jr.	5912
1	MS 1207	P. H. Eichel	5912
1	MS 1207	N. A. Doren	5912
1	MS 1207	I. A. Erteza	5912
1	MS 1207	T. S. Prevender	5912
1	MS 1207	P. A. Thompson	5912
1	MS 1207	D. E. Wahl	5912
1	MS 0328	F. M. Dickey	2612
1	MS 9018	Central Technical Files	8945-1
2	MS 0899	Technical Library	9616
1	MS 0612	Review & Approval Desk for DOE/OSTI	9612
1		Randy Bell	DOE NNSA/NA-22